Power and energy control strategies for a Vanadium Redox Flow Battery and wind farm combined system

Baccino, F.; Grillo, S.; Marinelli, M.; Massucco, S.; Silvestro, F.

Published in:
2nd IEEE PES International Conference and Exhibition on Innovative Smart Grid Technologies

Link to article, DOI:
10.1109/ISGTEurope.2011.6162658

Publication date:
2011

Power and Energy Control Strategies for a Vanadium Redox Flow Battery and Wind Farm Combined System

F. Baccino, S. Grillo, M. Marinelli, S. Massucco and F. Silvestro, *Members, IEEE*

***Abstract*-- The paper aims at describing two different control strategies for a combined system composed by a Vanadium Redox Flow Battery and a wind farm. A brief overview of the dynamic models used at describing the storage system and the wind turbines is presented. The focus is then devoted to the description of the two controllers, which task is to grant the desired power output at the point of connection of the system to the main network. The two control strategies called respectively *Power Control* and *Energy Control* are analyzed and their effectiveness is tested. The wind turbines are, in fact, fed with turbulent winds and the storage is controlled to perform a series of charges and discharges in order to have the desired global output. Their implementation and the dynamic simulations are performed in the Matlab-Simulink environment.**

***Index Terms*—Storage modeling, Vanadium Redox flow battery, Renewable generation.**

I. Introduction

THE development of the electric system, due to the strong increase of the distributed and renewable generation, is posing new challenges to the management and control of the power system. Concerning the wind generation, one of the major issues is related to its production profile, hardly predictable and manageable, that could cause overloading or overvoltage [1].

Thus the presence of a storage system could help to mitigate these drawbacks, allowing the full exploitation of the renewable energy sources. Nowadays the cost per stored energy is quite high and so it might not be economically feasible to install huge amount of batteries. The size of the storage systems can considerably vary and, depending on the size, different tasks can be performed as shown in [2]. They could perform duties ranging from power quality to primary frequency-power regulation and, in case of large storage sizing, compliance to day-ahead generation dispatching [3].

Each storage technology has some inherent limitations that make it practical or economical for only a limited range of applications. Though, the development of Vanadium Redox Battery (VRB) is expanding the possibilities for large-scale storage facilities, suitable for modern power systems. VRB have already been used in a number of demonstration applications and it is believed that the technology is close to being viable for a more widespread use [4].

The main advantages of the VRB reside in the long life and in the independence of energy and power ratings; moreover the design simplicity and ease of operation, due to the fact that the same electrolyte is used for both positive and negative side, make it a very interesting technology.

The paper is therefore aimed at presenting a VRB electrochemical dynamic model, a wind farm composed by five wind turbines and two different control strategies for the storage. The benefits and the problems of each control strategy are highlighted with the help of the simulations. The task of the control strategies, called *Power Control* and *Energy Control*, is to grant the desired output power of the system storage plus turbines, with special regard to the power profile and the energy profile respectively.

II. Dynamic Models

A. Storage Model

The flow battery converts the energy, stored in a liquid electrolyte, into electricity: the active material for both the positive and negative electrodes of the VRB is made up of vanadium ions that are dissolved in sulfuric acid and serve as metal ions with changing valence number.

The VRB system can be divided in three main components:

1. the fuel cell stack where the oxidation-reduction reaction is realized,
2. the two tanks where the electrolytes are stored,
3. the circulating system: pumps and pipes.

Fig. 1 reports a concept diagram of the VRB system: two controlled pumps move the electrolytes through the fuel cell and the rate of flowing determines the power generated or absorbed, while the total energy storage is determined by the size of the tanks. Therefore the total power available is related to the electrode area within the cell stacks, while the total storable energy is function of the tanks volume and of the electrolyte concentration [5], [6].

The VRB model proposed is suited for electrical studies and may have a general validity. The system modeled has a

F. Baccino, M. Marinelli, S. Massucco, F. Silvestro are with the *Department of Naval Architecture and Electrical Engineering*, University of Genova, Italy. E-mail: {francesco.baccino; mattia.marinelli; stefano.massucco; federico.silvestro}@unige.it

S. Grillo is with the *Department of Electrical Engineering*, Politecnico di Milano, Italy. E-mail: samuele.grillo@polimi.it

nominal power of 1.08 MW and a nominal energy of 10 MWh, it is composed of a set of 100 units, each with nominal values of 10.8 kW – 100 kWh; each unit is composed of 5 parallels of 40 cells connected in series. The nominal values of the single cell are 1.35 V and 40 A, determining thus a power of 54 W.

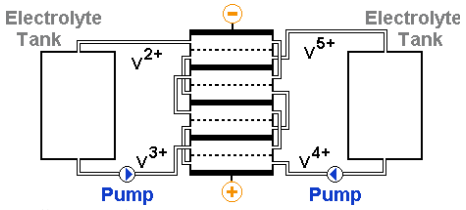

Fig. 1. Concept diagram of a VRB.

It is assumed that all the units are perfectly balanced and thus the tasks requested to the storage system are equally divided among them. Under this assumption all the dynamics are built in the single equivalent battery; the overall storage size is then obtained by multiplying/dividing the battery parameters for the number of series/parallel elements.

The modeled dynamics regard the State-of-Charge (SOC) behaviour, the electrochemical conversion and the limitations and protections systems. The main state variables are therefore the state of charge and the current: all the characteristic elements of the storage system (e.g., open circuit voltage, internal resistance and protection thresholds) present some kind of dependence from these state variables.

The block diagram reported in Fig. 2 can be understood reading it from the upper left to the lower right. The model input is the active power reference, *PrefBattery* (in pu or in W), that is the power that the battery is asked to release or to store. While the output, *PbatteryGrid*, is the power effectively produced, including the power required by the auxiliary systems and the losses in the Power Conversion System (PCS).

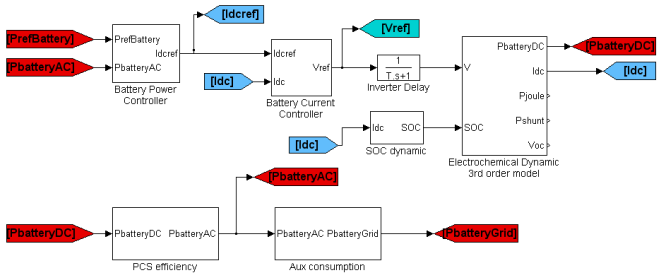

Fig. 2. VRB model block diagram.

The power reference is passed through a first controller stage that compares the request with the actual AC battery output (that mean the power at the PCS connection, before the pumps withdrawal): the output is the dc reference current. This new reference is passed through a second control loop, named Battery Current Controller, which sets the reference voltage that the DC side of the PCS has to set on the battery connection. Inside this control loop the extra signal, such as the max/min SOC level or max/min current trigger the blocking of the storage. The voltage applied, subject to a delay that models the PCS response time, is used in the Electrochemical Dynamic block to implement the storage dynamic model. A third order model has been used with two time constants in the equivalent electrical circuit as described in [7] and [8].

Finally the battery DC output is evaluated along with the internal shunt and Joule losses. By the knowledge of the converter efficiency curve and the auxiliary services consumption it is possible to compute the storage power transit towards the grid.

B. Storage economical analysis

A brief analysis of the storage technology cost is hereafter reported. Concerning the life of the storage it is assumed that after the expected charge/discharge cycles number and after the declared life-time the battery will still possess, at least, 80% of its nominal capacity.

Firstly the *SOC cycle* (or equivalent *SOC cycle*) is defined as the amount of energy that can be charged or discharged. Its value is equal to the nominal energy value of the storage. Thus an ideal charge from SOC level 0 to SOC level 1 means one *SOC cycle*. Similarly a charge from SOC level 0.5 to full charge and back to 0.5 means one SOC cycle. It is worth noting that the charge/discharge cycle number declared by the manufacturer is referred to a 80% discharge intensity, that means that a full charge and discharge goes from 0.2 SOC level to 1 and back to 0.2 corresponding thus to 1.6 *SOC cycles*.

The overall storage capital cost, C_c, is evaluated as the sum of a quota depending on the power capacity, P_c, due mainly to the cell and the PCS size, P_{nom}, and a quota depending on the energy size, E_c, i.e., the amount of Vanadium electrolyte, E_{nom}; finally the overall cost is multiplied by a constant factor of 1.2 to consider installation and designing costs [5]:

$$C_c = \left(P_c \cdot P_{nom} + E_c \cdot E_{nom} \right) \cdot 1.2 \qquad (1$$

The specific energy value, E_{value}, is calculated as the ratio between the capital cost and the total energy that the storage is declared to manage without significant aging (i.e. the nominal SOC cycles per the nominal energy) and the average roundtrip efficiency. This last parameter takes in account the fact that the energy, flowing inside and then outside the battery, will be subject to the internal Joule and shunt losses, the PCS efficiency and the pumps consumption; thus, the more intense are the charge and the discharge (i.e. the greater the power) the higher the losses. Of course the proposed models, can evaluate this kind of losses for the specific missions and thus estimate the real roundtrip efficiency. However a first evaluation is done considering the nominal battery efficiency equal to 80% per flow (meaning a roundtrip efficiency, *Eff*, around 64%):

$$E_{value} = C_c \Big/ \left(SOC_{cycles} \cdot E_{nom} / Eff \right) \qquad (2$$

A further correction requires the knowledge of the time length of the investments. The manufacturer states a useful life of 15 years without main maintenance operations, thus an horizon of 10 years for the return of the capital is assumed. The actualized energy value, E_{value_actual}, is thus calculated by the assumption of a discount rate, i, equal to 5%:

$$E_{value\_actual} = E_{value} \cdot \left[(1+i)^{y} \right] \quad (3$$

The main information concerning the battery data and costs are summarized in Table I. It can be seen that the actual specific cost determines an energy value of 72 €/MWh but this values is due to reduce in the next years if the forecasted technology improvements are achieved.

TABLE I
VRB COST ANALYSIS

Nominal size (Power – Energy)	1.08 MW – 10 MWh	
2007 specific costs [5] 2013 estimated specific costs [5]	2.3 $/W + 0.3 $/Wh 1.2 $/W + 0.2 $/Wh	
2007 capital cost 2013 estimated capital cost	6.36 M$ (= 4.54 M€*) 3.84 M$ (= 2.74 M€*)	
Nominal charge discharge cycles	15000 (= 1000 per year) equal to 24000 SOC cycles	
2007 Energy value actualized	101 $/MWh	72 €/MWh*
2013 Energy value actualized	61 $/MWh	44 €/MWh*
* change ratio equal to 1.4 $ per €		

C. Wind Farm

The wind turbine model realized is described from an electromechanical perspective, thus it provides: an analysis of the aerodynamic behaviour of the rotor including the pitch control system, the shaft dynamic and the maximum power tracking characteristic. The model is tuned for a 2 MW full converter direct drive equipped generator. This typology of wind turbine is characterized by the absence of the gearbox and the presence of AC/DC/AC converter sized for the whole power. Since the model is not intended to analyze dynamics faster than a fraction of second, there is no need to characterize in a detailed way the generation/conversion system, which thus is modeled as a negative load [9].

The rest of the electromechanical conversion system needs an accurate detail due to the interest in studying the possibility to reduce the output in certain conditions. There is, in fact, the need to model the delays introduced by the pitch controller and by the shaft rotational speed.

The block diagram that describes the main model components and their mutual interaction is depicted in Fig. 3. Reading the picture from left to right the first block met is the Aerodynamic one that evaluates the power harvested by the rotor that depends on wind speed, rotational speed and blade angle. This accelerating power, along with the rotational speed of the generator, enters the block named Shaft that describes the shaft behaviour and allows the evaluation of the power at the end of the shaft and of the turbine rotational speed. The blade angle is controlled by the Pitch Control that describes the dynamic of the pitch actuators.

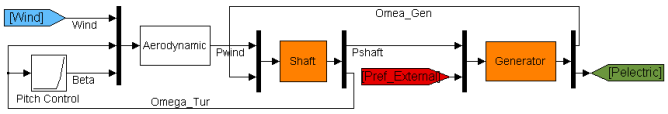

Fig. 3. Wind turbine model block diagram.

The five turbines are fed by different wind speeds profiles, shown in Fig. 4, calculated from the power output of five wind turbines belonging to a real wind farm. These data are five seconds sampled in order to better appreciate the wind turbulence. Their main information are reported in Table II.

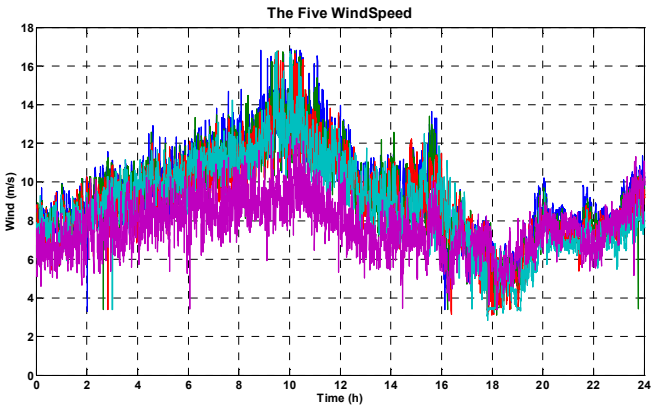

Fig. 4.The five wind speed profiles.

TABLE II
WIND SPEED CHARACTERISTIC PARAMETERS

	Wind 1 @ 90m	Wind 2 @ 90m	Wind 3 @ 90m	Wind 4 @ 90m	Wind 5 @ 90m
U max (m/s)	16.9	16.8	16.7	16.8	12.5
U media (m/s)	8.0	7.8	7.6	7.4	6.8
U min (m/s)	3.3	3.1	3.1	2.8	2.9
Turbulence Intensity	8.3%	8.6%	8.8%	8.8%	9.9%

III. WIND PARK LAYOUT AND CONTROL STRATEGIES

A. Wind Park Layout

As foretold, the idea proposed in this paper is to control the battery charging and discharging in order to control the whole plant power output at the Point of Common Coupling (PCC) [10]. An overview of the park layout is shown in Fig. 5 [11].

The five 2 MW wind turbines are identified by the blocks on the right side of the picture while the storage is located in the central block. The block that “calls” the wind speed profiles from the Matlab workspace is behind the picture of Eolo; while the measurements of the power transits and the power and energy references are included in the blocks just below Eolo’s one. The Wind Park Controllers (i.e. the Power and the Energy ones) are included in the greater block between the Eolo’s one and the storage’s one.

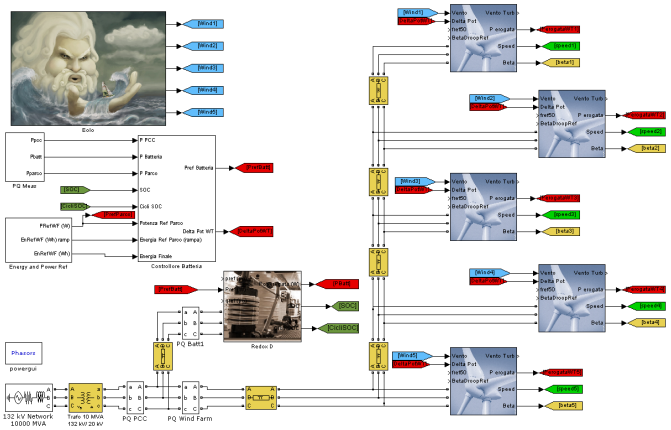

Fig. 5. Wind Park Layout.

B. Power Control

The first control strategy, named *Power Control,* has the task to set the reference power to the storage in order to compensate the wind farm fluctuations and to have at the PCC the desired power profile. This kind of control is very rigid: in fact, if a smooth power output (time frame of 1 second) is requested, the controller has to command a series of deep and very fast cycles of charge and discharge in order to compensate the fluctuation induced in the wind farm output by the turbulence. An excessive stress on the storage could be so realized and moreover an excess of energy depletion would result, due to the storage system losses, without taking a significant benefit to the system. If the main network is robust this kind of fluctuations could, in fact, be easily absorbed by the power system, or at least being compensated by other wind farms output, located somewhere else.

In order to avoid any blocking of the storage system due to maximum charge or minimum charge protection, it is present a feedback on the SOC [12]. The reference PCC power is thus summed to another power signal generated by a Power-SOC characteristic, as shown in Fig. 6.

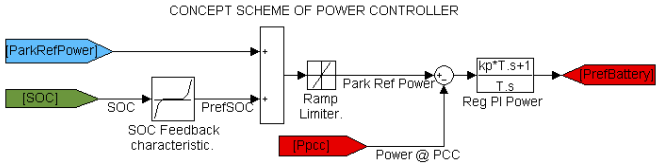

Fig. 6. Power controller block diagram.

This feedback reduces or increases the battery reference power with the purpose of keeping the SOC within an adequate range thus making the storage always available.

C. Energy Control

The second control strategy, named *Energy Control,* has thus been proposed. This control differs from the previous one because it is more elastic. The control action is realized within a longer time frame (i.e., 10 or 60 minutes instead of 1 second). As before, the desired power at the PCC is known, but it is not used in the control loop; it is used to compute the correspondent energy amount in the timeframe considered instead. This value is then equally divided in the time frame; it means that, for instance, at half of the period the farm is expected to have produced half the energy expected to be produced in the whole time frame. Thus the control loop uses the measure of the cumulated energy produced by the wind farm each second and compares it with the expected energy. If the produced energy is the same (or it is inside a certain band, e.g. ±10%) no charge/discharge actions are performed, otherwise the more the distance from the objective value, the deeper the charge/discharge is required.

The control strategy described in [13] for load management is thus realized in Simulink and suited to the storage management. The energy reference value, calculated as before using the forecasted power production, is the energy that the farm is expected to produce every ten minutes. This value is then used to create the control energy function, that means the blue curve depicted in Fig. 7.

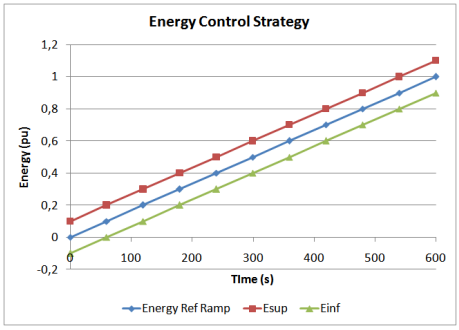

Fig. 7. Energy control strategy.

This time dependant value, is then compared with the cumulated energy produced by the farm. The control does not take any action if the two values are not coincident, but intervenes if the energy produced is above the red curve (the superior limit) or below the green one (the inferior limit).

The two curves (the red and the green one) form the control band and with this shape (i.e. parallel curves), there is no warranty that at the end of the period (i.e. at the 600th second) the energy produced will be equal to the reference value. This is due to the fact that this kind of control is a discrete-proportional type, thus a control action is taken if an error is generated but when the control variable is within the band (i.e. the control band) no corrective measurements are taken. If an integral action is intended to be realized the two curves can be designed to be convergent at the end (left picture of Fig. 8) or before the end (right picture of Fig. 8) of the control period.

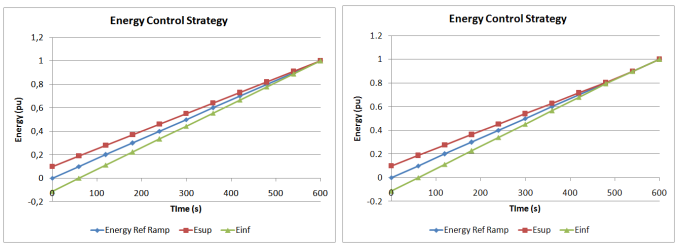

Fig. 8. Energy control strategies with integral action: end-convergent (left) and before-end-convergent or hybrid (right).

The realization in the Simulink block diagram is shown in Fig. 9. The relays shown generate a signal (respectively negative for a charge command and positive for a discharge command) when the error (in per unit) is above 0.

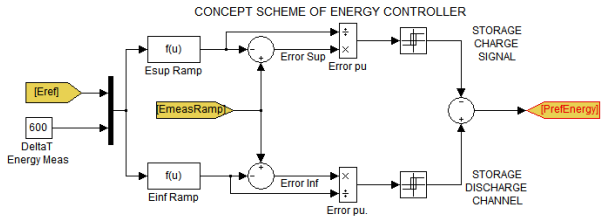

Fig. 9. Energy controller block diagram.

Both power and energy controllers, however, are intended to set a battery management in the short period (within the day). The power and the energy reference values could be the result of a scheduling established the day ahead by means of an optimal management algorithm. The main inputs for the optimization process would be the wind power forecast and the expected hourly energy price, the algorithm output (i.e. the hourly energy reference values) can then be tested in this Simulink model to prove its feasibility [14].

IV. Simulations

A. Power Control Strategy

Firstly the system behaviour with the *Power Control* enabled is analyzed. The first diagram of Fig. 10 shows the power production of the wind farm (red curve) and the smoothed transit at the PCC (blue curve) due to the instantaneous compensation provided by the VRB. The reference power, that means the forecasted mean power each 10 minutes without the effect induced by the local terrain turbulence, is shown in the second diagram of Fig. 10. The SOC-modified reference power is also present (blue curve) but it is superimposed to the previous one because the SOC-feedback is not triggered.

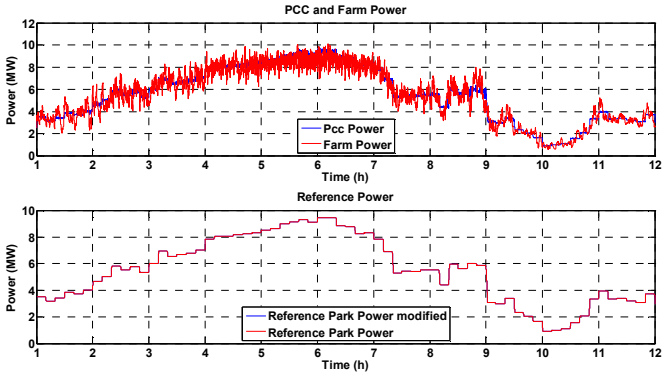

Fig. 10. PCC and Farm Power; Reference Powers.

The battery power output is reported in the first diagram of Fig. 11 along with the behaviour of the SOC level (shown in the second diagram). It can be seen that the SOC is going down and a longer simulation (i.e., 24h) would force the SOC feedback intervention.

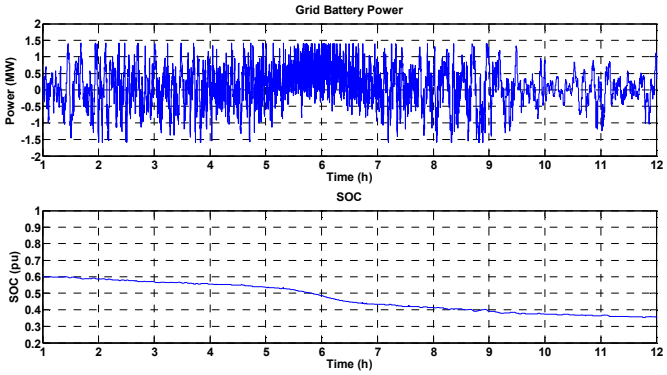

Fig. 11. Grid battery power; SOC.

Fig. 12 shows the correspondent energy production profiles each ten minutes. The typical saw-tooth profile is due to the fact that the energy measurement is performed within the ten-minutes period and it is reset to zero each time.

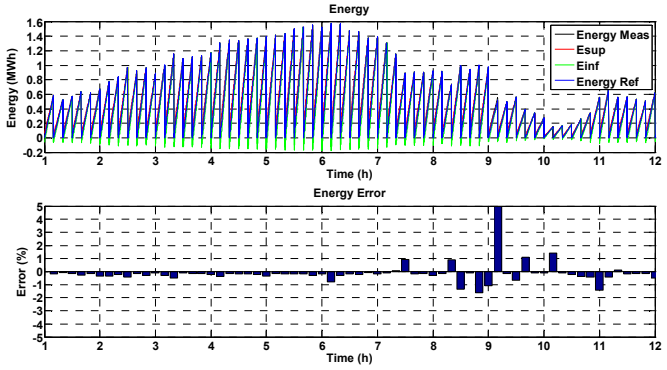

Fig. 12. Energy profiles; Energy errors.

The difference between the desired energy (Energy Ref, blue curve) and the cumulated one (Energy Meas, black curve), divided by the desired energy, is reported in the bar diagram (second diagram of Fig. 12).

B. Energy Control Strategy

This second scenario studies the system response to the Energy Control strategy. Fig. 13 reports, just like Fig. 10, the shape of the PCC power profile and the reference power each ten minutes. It can be graphically appreciated that the power profiles at the PCC (blue curve) is far from being smoothed (see also the PCC power deviation values in Table III).

The reason of that can be observed by the first diagram of Fig. 14, which reports the storage power profiles. This time the storage is not asked to compensate instantaneously the variability of the wind farm but just to grant, at the end of the ten-minutes window, the desired energy amount. Thus the storage is required to perform a less stressing task.

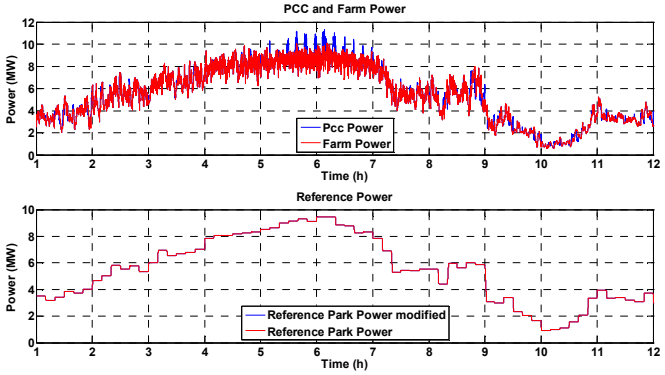

Fig. 13. PCC and Farm Power; Reference Power.

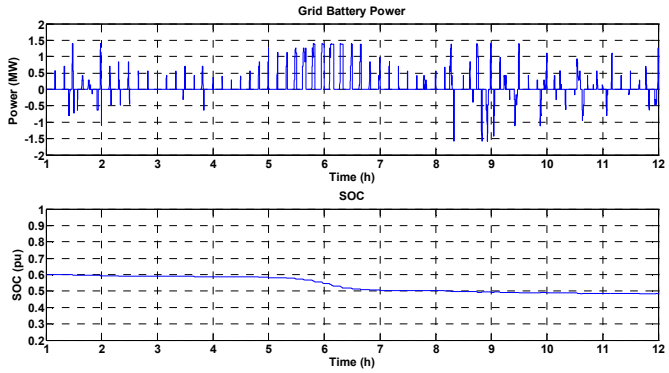

Fig. 14. Grid battery power; SOC.

The energy profiles, along with the correspondent energy errors, are reported in Fig. 15.

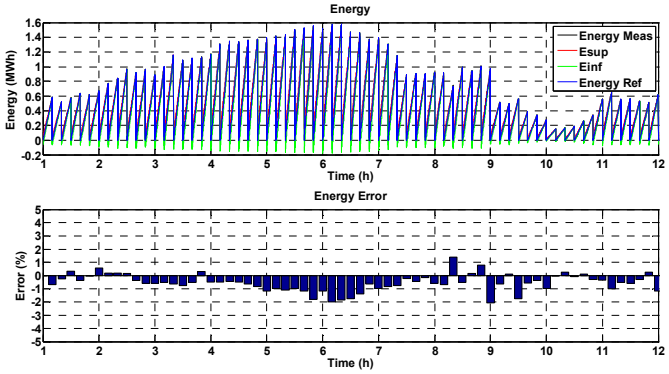

Fig. 15. Energy profiles; Energy errors.

In order to better appreciate how the energy controller works a zoom of one period is reported in the first diagram of Fig. 16. The second one shows the charge/discharge action of the storage instead.

This control strategy has been realized with the control path reported in the left picture of Fig. 8. The same analysis is performed also with the path shown in the right picture, which forces the control bands to reach the convergence point at the 8th minutes instead of the 10th. The numerical results are reported in the last column of Table III along with the results of the just illustrated scenarios.

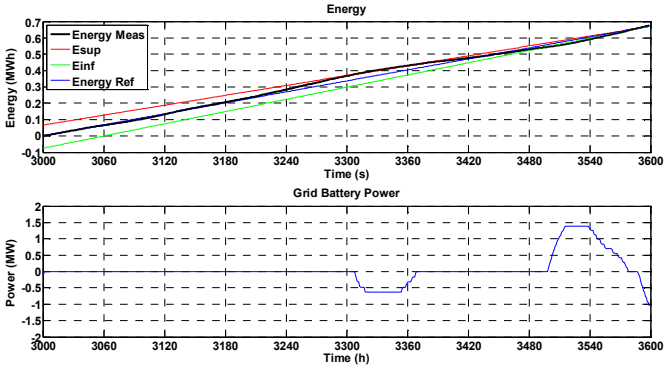

Fig. 16. Energy profile; Grid battery power.

C. Results Comparison

The overall results for the three set of simulations are reported in Table III. It can be seen that the *Energy Control* strategies do not grant a smooth power profile at the PCC but are able to grant the same desired PCC energy without excessive battery work (i.e. *SOC cycles* or charge/discharge cycles).

The average energy error is about 0.44% in case of the *Power Control* and goes up to 0.64% with the first *Energy Control* strategy. It can be noted that the anticipation of the convergence point of the control band before the end of the ten minutes window (i.e., in the *Energy Hybrid* scenario) allows the storage to better pursue the desired energy value and thus the average energy error goes down to 0.37%.

The subsequent variables reported in table III are defined as follows. The Mean Power deviation is the mean of the 72 ratios (i.e., 6 periods per 12 hours) between the ten minutes period standard deviation of the power transit and the period average value:

$$I_p = \sum_{i=1}^{72} \sigma_P\big|_{t=600} \Big/ \bar{P}\big|_{t=600} \Big/ 72 \qquad (4$$

The *Battery Works* are the sum, without sign of the released and the stored energies. While the *SOC cycles*, already introduced in the economical analysis paragraph, is the ratio between the *Battery Work (DC)* and the nominal energy:

$$SOC\_cycles = \int |P_{dc}| \bullet dt \Big/ E_{nom} \qquad (5$$

The different efficiencies are referred to different parts of the storage system. Fig. 17 can help to understand these efficiency areas. *Eta DC* is useful to analyze the electrochemical performances of the storage, thus it includes the Joule and the shunt losses. *Eta AC* measures the PCS efficiency, while *Eta pumps* gives the measure of the consumption of the main auxiliary system present (i.e., the circulating pumps) compared to the power transit inside and outside of the storage. The *Eta system* is the global product of the efficiencies just described.

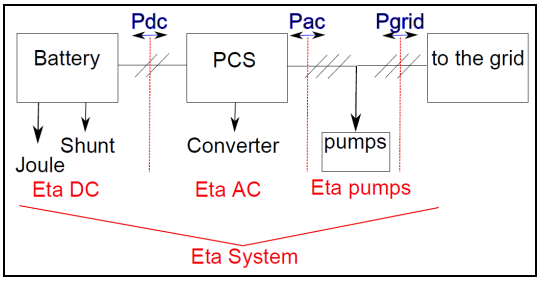

Fig. 17. Battery system efficiencies definition.

TABLE III
RESULTS COMPARISON (12 HOURS PERIOD)

Park Result	**Power Ctrl**	**Energy Ctrl**	**En. hybrid Ctrl**
Farm Energy (MWh)	64.075	64.075	64.075
PCC Energy (MWh)	65.143	64.854	65.095
Ref Energy SOC-Revised (MWh)	65.192	65.192	65.192
Ref Energy (MWh)	65.192	65.192	65.192
Mean Ref Power (MW)	5.433	5.433	5.433
Farm Mean Power Deviation	11.79%	11.79%	11.79%
PCC Mean Power Deviation	1.80%	11.86%	11.79%
Average Energy Error (%)	0.44%	0.64%	0.37%
Battery Result DC Side	**Power Ctrl**	**Energy Ctrl**	**En. hybrid Ctrl**
DC Battery Work (MWh)	5.566	1.321	2.378
DC Stored Energy (MWh)	1.917	0.192	0.537
DC Released Energy (MWh)	3.649	1.129	1.841
Number of SOC cycles (pu)	0.557	0.132	0.238
Delta SOC (pu)	-0.173	-0.094	-0.130
Battery Result Grid Side	**Power Ctrl**	**Energy Ctrl**	**En. hybrid Ctrl**
Max Power (MW)	1.500	1.500	1.500
Grid Battery Work (MWh)	5.349	1.209	2.220
Grid Stored Energy (MWh)	2.140	0.215	0.600
Grid Released Energy (MWh)	3.209	0.994	1.620
PCS load factor (%)	29.7%	6.7%	12.3%
Battery losses	**Power Ctrl**	**Energy Ctrl**	**En. hybrid Ctrl**
Joule losses (MWh)	0.489	0.169	0.289
Shunt losses (MWh)	0.179	0.046	0.081
Converter losses (MWh)	0.283	0.067	0.120
Aux losses (MWh)	0.380	0.090	0.162
Storage global losses (MWh)	1.332	0.372	0.653
Efficiencies	**Power Ctrl**	**Energy Ctrl**	**En. hybrid Ctrl**
Eta DC (Joule&Shunt)	92.6%	95.9%	95.1%
Eta AC (Converter)	95.0%	95.0%	95.0%
Eta pumps (Aux)	91.7%	81.6%	83.8%
Eta system	80.7%	74.4%	75.7%

Particular attention must be given to the way of defining the efficiency. Generally the system efficiency is the ratio between the output energy and the input energy. But, due to the reversibility of the storage, the way of computing the efficiency changes. The different formulas are hereafter reported:

$$\begin{cases} P_{DC} \geq 0 \rightarrow \eta_{DC} = P_{DC} \Big/ \left(P_{DC} + P_{joule} + P_{shunt}\right) \\ P_{DC} < 0 \rightarrow \eta_{DC} = \left(P_{DC} - P_{joule} - P_{shunt}\right) \Big/ P_{DC} \end{cases} \quad (6$$

$$\begin{cases} P_{AC} \geq 0 \rightarrow \eta_{AC} = P_{AC} \Big/ P_{DC} \\ P_{AC} < 0 \rightarrow \eta_{AC} = P_{DC} \Big/ P_{AC} \end{cases} \quad (7$$

$$\begin{cases} P_{Pumps} \geq 0 \rightarrow \eta_{Pumps} = P_{Grid} \Big/ P_{AC} \\ P_{Pumps} < 0 \rightarrow \eta_{Pumps} = P_{AC} \Big/ P_{Grid} \end{cases} \quad (8$$

$$\eta_{System} = \eta_{DC} \bullet \eta_{AC} \bullet \eta_{Pumps} \quad (9$$

It is interesting to note that the efficiency passes from around 90%, when just considering the specific battery losses, to 80% once all the system losses are included. Similar trends can be observed also in the cases of the *Energy Controls*.

The lost energy is about 1.33 MWh in the *Power Control* scenario while it is reduced to 0.65 and 0.37 MWh in two *Energy Control* scenarios, corresponding to respectively 2%, 1% and 0.6% of the farm production (that is around 64 MWh) in the 12 hours simulation. It is thus necessary to establish if the improvement, and moreover the kind of improvement, in the power quality balances the minor energy production.

It is also necessary to pay attention to the number of *SOC cycles* (0.55 in case of the most stressing scenario) that could lead to premature aging of the storage. In fact, if it is assumed that the simulated work cycle is a good representation for every other day of the year, this would lead to an overall number of 400 cycles per year. As foretold VRB manufacturers claims for 1600 SOC cycles (corresponding to 1000 cycles of charge/discharge) per year, thus the requested mission could be satisfied without particular problems.

Last but not least, the rapidity or step response must be considered. From this point of view the VRB offers extraordinary speed: if the pumps are already running it can commute from maximum charge to maximum discharge within few seconds; the start-up (i.e. when everything is shut down) requires just few minutes of electrolyte pre-mixing, before the system is fully ready.

V. CONCLUSIONS

The present paper focused on the development of models of wind turbines and storage systems, in Matlab-Simulink environment, useful for implementing integrated control strategies of the whole resulting system in order to describe the benefits that storage can provide to renewable generation. The main purpose was the facilitation of the integration of distributed, intrinsically not dispatchable, generation in the electric grid.

The electrochemical dynamic model of a Vanadium Redox Flow battery and the electromechanical dynamic model of five wind turbines have been briefly presented. The wind turbines used five wind speed profiles with a detail of five seconds.

Three control strategies have been envisaged, the first one named *Power Control*, the second one *Energy Control* and the

last one *Energy Hybrid Control* with the aim of setting the battery charging and discharging phases in order to control the whole plant output.

It was thus highlighted how the storage system could grant benefits in term of controllability of the wind park output. However, the rigid *Power Control*, whose aim was to pursue a perfectly smoothed output, proved to be quite stressful for the storage and energy-depleting. Both the *Energy Control* strategies allowed a smarter management of the storage, granting the desired energy production at the PCC, without, however, any particular regard to the smoothness of the overall generated power profile.

Future works will focus on the coupling of the storage system with photovoltaic power plants too. The testing of these control strategies on real small devices will be implemented later in the year.

VI. References

[1] A. Neural, V.I Kogan, C.M. Schafer C.M., "Load Leveling Reduces T&D Line Losses", *Power Delivery, IEEE Transactions on*, vol. 23, no. 4, pp. 2168–2173, Oct. 2008

[2] R. Fioravanti, K. Vu, W. Stadlin, "Large scale solution", *Power and Energy Magazine, IEEE*, vol. 7, no. 4, pp. 48-57, July-Aug. 2009

[3] A. Oudalov, D. Chartouni, C. Ohler, G. Linhofer, "Value Analysis of Battery Energy Storage Applications in Power Systems", *Power Systems Conference and Exposition, PSCE '06. 2006 IEEE PES*, pp.2206-2211, Atlanta, Oct. 29 - Nov. 1 2006

[4] T. Shigematsu, T. Kumamoto, H. Deguchi, T. Hara, "Applications of a Vanadium Redox-flow Battery to Maintain Power Quality", *Transmission and Distribution Conference and Exhibition 2002*, Yokohama, 6-10 Oct. 2002.

[5] Vanadium Redox Flow Batteries: An In-Depth Analysis. EPRI, Palo Alto, CA: 2007. 1014836.

[6] C. Blanc, A. Rufer, "*Multiphysics and Energetic Modeling of a Vanadium Redox Flow Battery*", IEEE International Conference on Sustainable Energy Technologies 2008, pp. 696-701, Singapore, 24-27 Nov. 2008.

[7] M. Chen and A. Rincon Mora, *"Accurate Electrical Battery Model Capable of Predicting Runtime and I–V Performance"*, IEEE Transaction on Energy Conversion, vol. 21, no. 2, pp. 504-511, Jun. 2006.

[8] E. Micolano, M. Broglia, L. Mazzocchi and C. Bossi, "*Sviluppo di modelli di sistemi di accumulo di tipo tradizionale ed avanzato per impieghi nella generazione distribuita al fine della loro rappresentazione in sistemi complessi (Traditional and advanced storage system models development for embedded generation uses in complex systems studies)"*, GENDIS Technical Report A5-053120, pp.1-51, RSE (former CESI), Milano, Dec. 2005.

[9] A. Hansen, F. Iov, P. Sørensen, N. Cutululis, C. Jauch and F. Blaabjerg, *"Dynamic wind turbine models in power system simulation tool DIgSILENT"*, Risø-R-1400 ed.2, pp. 1-190, Risø National Laboratory, Roskilde, Aug. 2007.

[10] T. Funabashi, Y. Kikunaga, A. Y. Saber, H. Sekine, T. Senjyu and A. Yona, *"Coordinate Control of Wind Turbine and Battery in Wind Power Generation System"*, IEEE Power and Energy Society General Meeting, pp. 1-7, Pittsburgh, 20-24 Jul. 2008.

[11] S. Grillo, M. Marinelli and F. Silvestro (2011). Wind Turbines Integration with Storage Devices: Modelling and Control Strategies, Wind Turbines, Ibrahim Al-Bahadly (Ed.), ISBN: 978-953-307-221-0, InTech, Available from: http://www.intechopen.com/articles/show/title/wind-turbines-integration-with-storage-devices-modelling-and-control-strategies.

[12] K. Yoshimoto, T. Nanahara, G. Koshimizu, *"Analysis of Data Obtained in Demonstration Test about Battery Energy Storage System to Mitigate Output Fluctuation of Wind Farm"*, Cigré/IEEE PES Joint Symposium, pp. 1-6, Calgary, 29-31 Jul. 2009.

[13] IEEE Standard, *"IEEE Recommended Practice for Energy Management in Industrial and Commercial Facilities"*, IEEE Std 739-1995, pp. 1-297, 1996.

[14] A. Oudalov, D. Chartouni and C. Ohler, *"Optimizing a Battery Energy Storage System for Primary Frequency Control"*, IEEE Transactions on Power Systems, Vol. 22, No. 3, pp. 1259-1266, Aug. 2007

VII. Biographies

Francesco Baccino was born in Genova, Italy, in 1986. He received the Master degree in electrical engineering in 2010 and is currently pursuing the Ph.D. degree in power systems, both from the University of Genova. His research interests regard smartgrids, focusing on the optimal integration of RES, DG, storage and PEV.

Samuele Grillo was born in Alessandria, Italy, in 1980. He received the "Laurea" degree in electronic engineering in 2004 from the University of Genova and, from the same University, a Ph.D. in power systems in 2008. From February 2008 to June 2010 he has been holder of a research grant at the University of Genova. From July 2010 he is assistant professor at Politecnico di Milano. His research interests regard optimization and control techniques, smart grids, neural networks and their application to power systems (i.e., security assessment, load and production forecast, local and small generation management).

Mattia Marinelli was born in Genova, Italy, in 1983. He received the Master degree in electrical engineering in 2007 and the European Ph.D. in power systems in March 2011 both from the University of Genova. He is currently holding a post-doc contract. His research interests regard wind and solar data analysis, distributed generators (mainly wind turbines) electromechanical and electrochemical storage modeling for integration studies of renewable energy sources in power systems.

Stefano Massucco received the Doctor degree in electrical engineering at the University of Genova, Italy, in 1979. From 1979 to 1987, he had been working at the Electrical Engineering Department of Genova University, at CREL - the Electrical Research Center of ENEL (Italian Electricity Board) in Milano, Italy, and at ANSALDO S.p.A. in Genova, Italy. He has been Associate Professor of Power Systems at the University of Pavia and since 1993 at the Electrical Engineering Department, University of Genova, as Full Professor since 2000. His research interests are in power systems and distributed generation and smartgrids modeling, control, and management. Member of CIGRE Working Group 601 of Study Committee C4 for "Review of on-line Dynamic Security Assessment Tools and Techniques".

Federico Silvestro was born in Genova, Italy, in 1973. Received the degree in electrical engineering from the University of Genoa in 1998 and the PhD degree from the same University in power systems in 2002, with a dissertation on artificial intelligence applications to power systems. He is now Assistant Professor at the Dept. of Naval Architecture and Electrical Engineering, University of Genova, where he is working in power system simulators, security assessment, knowledge based systems applied to power systems and distributed generation.